The Thesis Committee for Andrew Clayton Stier
Certifies that this is the approved version of the following thesis:

Smart Epidermal Heater with On-Site Temperature Feedback Control

APPROVED BY
SUPERVISING COMMITTEE:

Supervisor:

Nanshu Lu

Kenneth Diller

Quick-Fabrication Epidermal Electronic Heater with On-Site Temperature Feedback Control

by

Andrew Clayton Stier, B.S.

Thesis

Presented to the Faculty of the Graduate School of

The University of Texas at Austin

in Partial Fulfillment

of the Requirements

for the Degree of

Master of Science in Engineering

The University of Texas at Austin

May 2016

Dedication

I dedicate this thesis to my loving parents, who support me and inspire me in all my endeavors.

Acknowledgements

First and foremost, I would like to acknowledge my advisor Dr. Nanshu Lu, who has guided, motivated, and inspired me throughout this research project. I would like to acknowledge Dr. Kenneth Diller, whom without I would have never found this project, for all of the advice and the resources that he has provided. I would like to acknowledge Eshan Halekote, who has been a great companion in completing this project and has put in a significant amount of valuable work. I would like to acknowledge Rocky Yang for his advice and guidance concerning the figures in my thesis as well as for being the photographer for many of the photos. I would like to acknowledge Andrew Mark for his work on the PID controller algorithm and his guidance in adapting it for my device. I would like to acknowledge Shutao Qiao for his help with the theoretical analysis of the device. I would like to acknowledge Dr. Jonathan Valvano for his advice and troubleshooting tips. Finally I would like to acknowledge all of the members of the Lu Biointegrated Electronics group, who have all been brilliant peers, supportive companions, and great friends.

Abstract

Quick-Fabrication Epidermal Electronic Heater with On-Site Temperature Feedback Control

Andrew Clayton Stier, M.S.E.

The University of Texas at Austin, 2016

Supervisor: Nanshu Lu

Smart wearable heaters can serve many important roles in the medical field, including thermal joint therapy, controlled transdermal drug delivery, and perioperative warming. Currently existing heaters are too bulky, rigid, or difficult to control to be used as wearable and mobile devices. There has been progress in the development of stretchable, conformable heaters, but they currently take significant time to produce. Also, they all lack sufficient temperature feedback control, which is necessary to accommodate the dynamic temperatures of the human epidermis and prevent burning. We present a cost-effective epidermal electronic heater that can be produced by the cut-and-paste method and has autonomous temperature control using on-site temperature feedback. The device comprises a heater layer and a resistance temperature detector (RTD) layer on a stretchable medical tape. The total thickness is less than 70 μm and the stretchability and stiffness are on par with human epidermis. We demonstrate the device's ability to maintain specific temperatures over extended durations of time and accurately switch between different target temperatures without any prior knowledge of

the relationship between power supplied to the heater and what temperature the skin will reach.

Table of Contents

List of Tables x

List of Figures xi

Chapter 1: Introduction 1

Need For Wearable Heaters 1

Joint Therapy 1

Perioperative Warming 1

Drug Release Control and Acceleration 3

Current Heaters 3

Stretchable Wearable Heaters 4

Heater Feedback Control 6

Our Device 7

Chapter 2: Materials and Methods 9

Heater Materials 9

Cut-and-Paste Fabrication Process 9

Snap-Button Connection and Final Layer 11

Hot-Plate Calibration 13

Calibration on Glass 14

PID Test on Glass 16

Materials and Methods Conclusion 17

Chapter 3: Results and Discussion 18

Conformability 18

Calibration on Skin 19

PID Control on Skin 22

Power Density Calculations 23

Stretchability 26

Results Conclusion 30

Chapter 4: Conclusion..31

References..34

List of Tables

Table 1: Power consumptions of different heaters from literature. 26

List of Figures

Figure 1. PID Control Block Diagram 7
Figure 2: Fabrication of Device.. 11
Figure 3: Connections 13
Figure 4: Hotplate Calibration. 14
Figure 5: In-Situ Calibration Set-up.. 15
Figure 6: Preliminary Tests on Glass.. 16
Figure 7: PID Control Circuit Set-up. 17
Figure 8: Conformability Results. 19
Figure 9: Calibration on Skin. 21
Figure 10: PID Results on Skin. 23
Figure 11: Power Consumption Characterization. 25
Figure 12: Stretchability Tests. 29

Chapter 1: Introduction

There exists a need for stretchable, conformable electronic heating devices which can conform to skin. Such devices can serve a variety of applications in the medical field. In this chapter, I will lay out the various applications of wearable heaters, the heaters currently used for these applications, the new advances in wearable heater technology, and finally introduce the wearable heater technology that I have developed.

NEED FOR WEARABLE HEATERS

Joint Therapy

Joint injuries are common and can be caused by obesity, occupational overuse, disease, or age. These injuries can have many undesirable symptoms, including pain, restriction of movement, edema, and inflammation and swelling.[1] Joint injury is also a risk factor for osteoarthritis[2].

A classic treatment for joint injuries is thermal therapy. Heating joint injuries expands the vascular systems surrounding the joint to expand. This increases blood flow to the collagen tissue surrounding the joint. This in turn increases flexibility of the ligament, reduces pain, and may help reduce the injury[1,3–5].

Perioperative Warming

The anesthesia used in surgeries today interferes with the body's thermoregulatory system, which, when combined with the cold temperatures of operating rooms, causes patient hypothermia. This hypothermia causes significant complications with the patient's biological systems and the surgery[6].

Recent studies have suggested the possibility for an efficient method for warming the body during surgery by considering the biological process by which perioperative hypothermia occurs. Non-hairy surfaces of the skin, also referred to as glabrous skin surfaces, contain specialized structures for heat exchange called venous plexuses. Examples of glabrous skin surfaces include skin on the palms of the hands, the soles of the feet, ears, cheeks, forehead, and nose. These venous plexuses, which lie basal to these skin surfaces, deliver large amounts of blood to the surface of the skin when the body vasodilates. They do this by shunting blood directly from the arteries to the surface of the skin through vessels called arteriovenous anastamoses, which bypass the capillaries. The mass volumes of blood that the venous plexuses bring to the skin surface allow for a large amount of heat exchange between the blood and the environment.[7] Perioperative hypothermia occurs when the anesthesia induces vasodilation and thus heat exchange with the cold operating room through the venous plexuses.

Knowing this, it has been proposed that the hypothermia can be counteracted by warming the glabrous skin surfaces while the blood vessels are distended[7]. However, there are some challenges in accomplishing this. In order to heat the entire body while only covering relatively small surface area, large amounts heat must be transferred quickly and efficiently. The most effective form of heat transfer is conductive heating through a solid[8]. However, typical solid materials cannot bend and stretch with the skin and therefore cannot maintain consistent contact. Heating the body would require using the heating device near the maximum temperature possible without causing damage or pain to the patients[9]. If the heating device does not maintain consistent contact, the parts of the device not touching the skin could heat up to temperatures over that maximum and cause damage or pain when they reestablish contact with the skin[10].

Drug Release Control and Acceleration

Under normal conditions, skin is able to repair and heal itself. However, if the skin is damaged badly through a laceration, burn, or infection, the skin is not able to carry out this function and needs the help of medication[11]. The blood vessels leading to the wound can be too damaged to supply medication taken orally to the wound site, and large amounts of medicine must be administered to compensate for this, which could lead to toxicity[12]. An alternative method of medication is to apply drugs topically to the wound site. Ideally, the drugs can be administered in a controlled manner such that the drug is released at desired times and held at other times[13]. Aside from skin wounds, controlled drug release through the skin would provide a non-invasive and convenient way to take drugs in a controlled manner. The rates and times of the drug release can even potentially be controlled autonomously based off of readings taken from an epidermal device.[14]

A heater can be used to enable this control of drugs from an epidermal patch. Drugs can be stored in a substance which only releases the drug when it is heated. Also, once the drugs are released to the skin, heat can accelerate the rate at which the drug penetrates through the skin. It has been shown that m-silica nanoparticles work effectively to store drugs and deliver them when heated, and that the diffusion of these drugs through the skin will increase when heated.[14] Controlled drug containment and heat-induced release has also been successfully demonstrated with Poly N-Isopropylacrylamide hydrogels.[13]

Current Heaters

The technology of dermal patches that can release growth factors and drugs on demand is relatively new, and there is not yet any commercially available drug-release patch with an integrated heater[13]. Conventional heaters used for joint injuries include electric heat packs[5] and heat wraps[15]. Heat packs do not have very controllable

temperature and are heavy and bulky. Heat wraps are easier to control but are also heavy, and their rigidity makes it difficult for them to be worn seamlessly[4]. Besides making the device less comfortable, the wearability issues can also cause problems with complete adhesion. Lack of uniform and consistent adhesion to the skin surface could lead to air gaps which cause hot spots[10]. These hotspots could burn the skin if the heater is operated near the safety threshold of 43°C[8]. This can severely limit the range and thus the effectiveness of the heater. Perioperative warming by heating the glabrous skin, for example, uses a heater set at 42°C[9].

One heating method that can safely heat the body at high temperatures, and the current gold standard for preventing the hypothermia cause by anesthesia, is forced air warming. Forced air warming heats air and pumps it into blankets covering large portions of the patient. While effective at raising the core body temperature, forced air warming has some disadvantages. The surgical field must be left exposed and thus does not benefit from the warming effects of the device, and specially shaped blankets for specific surgeries are expensive and not readily available[16]. Additionally, there is some time lag between administering the anesthesia and heating the patient due to having to wait for the surgical draping to be completed. Lastly, the forced air warming apparatus is bulky, and requires moderate storage space.[17]

STRETCHABLE WEARABLE HEATERS

Recently there has been an expansion of the new technology of stretchable electronics. Some examples of methods that have been used to produce these type of electronics include elastomers made conductive by embedding carbon nanotubes (CNTs)

in them[18,19], chemically bonding silver flakes to CNTs[20,21], combining silver nanoparticles and elastomeric fibres[22], constructing stretchable Au electrodes from multi layers of Au nanosheets[23], depositing silver nanoparticles in polyeruthane[4,24], and patterning conductive materials into serpentine or fractal shapes to minimize their strain during stretching. This last method results in devices referred to as epidermal electronics. Epidermal electronics are ultrathin, ultrasoft electronics that are fabricated in such a way that they can adhere and conform to skin surfaces and bend and stretch without breaking, detaching, or imposing any mechanical constraint to the skin [25–27].

In recent years progress has been made specifically in the area of stretchable heaters, including joule heating devices fabricated from composite silver nanowires[4,28] and epidermal electronics with a heating element composed of Au[4,9,27,28]. Using a solid conductive heater in the form of an epidermal electronic could solve the major disadvantage of typical solid heaters. However, these stretchable heaters involve expensive or time consuming procedures to produce. Moreover, most of them have no method of acquiring temperature feedback from the heater as they are not equipped with any temperature sensors. The stretchable heaters that do have temperature feedback use the device's heating element itself to perform the temperature detection[14,29]. This results in a reading of the average temperature across the entire range of the heater. This does not allow for measuring temperature at specific areas of the heater. In cases where the heat distribution is not completely uniform, such as is the case with these heaters, an average reading across the entire range of the heater is not optimally specific and accurate.

Moreover, none of the heaters except for one use temperature feedback to autonomously control the temperature of the heater. The one heater that does only has it as a safety switch which turns the heater off if it gets too hot- aside from that, the temperature feedback is not used to actively control the heat of the heater[14]. Without the use of effective temperature feedback, past stretchable heating devices have relied on the relationship between voltage and heat generated in order to maintain the heater at a desired temperature. However, conditions vary from person to person, and it is inaccurate to assume a consistent relationship between voltage and temperature if you wish to apply the same heater to multiple subjects. For example, changes in blood flow can cause changes in epidermal skin temperature[9].

HEATER FEEDBACK CONTROL

Proportional-integral-derivative (PID) control is the most common algorithm for controlling something based on feedback. A block diagram of the closed-loop system with PID control is shown in Figure 1. In this algorithm, a setpoint, *r*, is given that the device should be at. In the case of a heater, *r* is the temperature that should be reached due to the heater. At each iteration of the loop, the error, *e*, is calculated by taking the difference between the current state of the device, *y*, and *r*. The control signal, *u*, is then calculated using the integral, the derivative, and a constant proportion to the error *e* as can be seen in the following equation:

$$u = k_p e + k_i \int_0^t e(\tau)d\tau + k_d \frac{de}{dt} \quad (1)$$

Where k_i, k_p, and k_d are constants set by the designer which determine how much of an influence each term in the equation should have. The derivate term is often set to zero.[30]

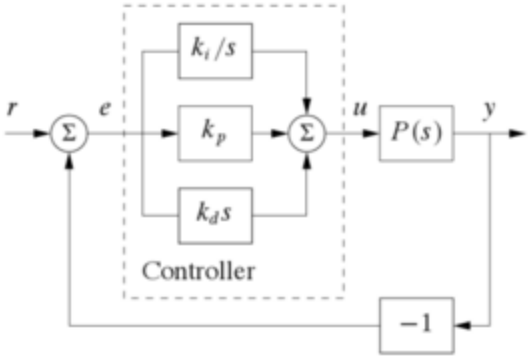

Figure 1. PID Control Block Diagram[30]

OUR DEVICE

The recently developed cut-and-paste method[31], in which patterns are cut out of ultrathin metals and transferred to an adhesive substrate, allows for cheaper, quicker, more efficient fabrication of epidermal electronics. This method also allows for the use of cheaper metals which are more difficult to incorporate using typical nanofabrication methods.

Here we present an inexpensive, easy to fabricate, and power efficient epidermal electronic heating device with temperature feedback fabricated from aluminum and gold using the cut-and-paste method. Included with this is a software system which uses temperature feedback control to maintain the heater at a desired temperature. This heater

is able to maintain a consistent and relatively uniform heat distribution over a large area for extended periods of time.

Chapter 2: Materials and Methods

In this section I will discuss the materials that were used to fabricate the heater, the method for how the device and its connections were created, and the methods for the preliminary tests that were run.

HEATER MATERIALS

The heater consists of an aluminum resistive heating element and a gold resistance temperature detector (RTD) printed onto a Tegaderm thin patch using the cut and paste method. The tegaderm patch is thin, stretchable, and adhesive. The heating element is made out of 7μm/13μm Al/PET, with the aluminum side facing the tegaderm and the PET side facing out. The PET allows for increased stretchability and electrical insulation. The aluminum is a thick, cheap, low resistance metal which dissipates power in the form of heat when current runs through it. The RTD is made out of 100nm/15nm/13μm Au/Cr/PET, with the PET facing the patch and the gold facing out. This results in two layers of insulation between the heater and the RTD.

CUT-AND-PASTE FABRICATION PROCESS

In order to make the heating element, the Al/PET was rolled onto thermal release tape (TRT) with the PET side facing the TRT. The TRT was then placed on the cutting mat of a Silhouette Cameo Electronic Cutting Machine, which was then inserted into the machine. A 2D pattern designed in SolidWorks was then imported into Silhouette Studios and cut out of the material. The TRT was taped to a wax sheet and placed on a hotplate for 5 minutes at a heat of 120°C. The sheet helped keep the material from popping off of the TRT as it was heated and lost its adhesiveness. The TRT was then taken of the hotplate, the wax sheet as removed, and tweezers were used to peel off all of the excess Al/PET apart from the pattern that we had cut into it. We then placed the adhesive side of

a Tegaderm patch onto the pattern to peel the pattern off of the TRT and onto the Tegaderm. The Al/PET pattern was thus transferred to the tegaderm with the Al side facing the tegaderm and the PET side facing out (Figure 2A).

In order to make the material for the RTD, 13µm PET was taped around 3in. x 1in. x 1mm glass slides and then sprayed with acetone, IPA, and water, then blown dry with compressed air. 10nm of chromium and then 100nm of Au were then sputtered onto the PET. The tape attaching the PET to the glass slides was then removed. The Au/Cr/PET was then put through the same process as the Al/PET with a different pattern cut into it, and transferred on top of the aluminum with the PET side facing the tegaderm and the Au side facing out (Figure 2A). The final result can be seen in Figure 2B.

Both the heater and the RTD were cut into a serpentine pattern, which maximizes stretchability. Specifically, the stretchability of these serpentines is maximized by fabricating their width to be as narrow as possible[25], which, due to the resolution of the cut-and-paste method, is 200µm[31].

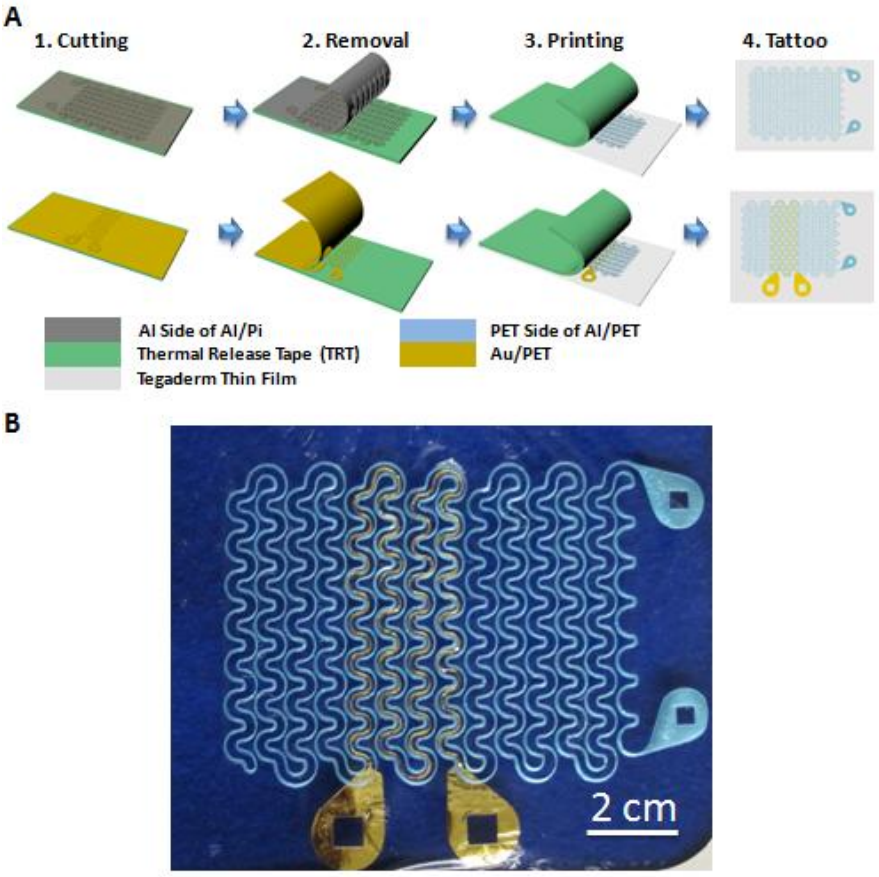

Figure 2: A) Fabrication process used for heater and RTD. Material is put on thermal release tape (TRT) and cut with Silhoutte cutter. TRT is heated, excess material is removed, and remaining material is transferred to Tegaderm. B) Complete device on tegaderm. Aluminum with blue polyimide backing forms the resistive heating element while Au/Cr 100/10 nm forms the resistance temperature detector.

SNAP-BUTTON CONNECTION AND FINAL LAYER

Connections to the heater are made using snap buttons. The aluminum (Al) heating element and the gold (Au) resistance temperature detector (RTD) each have two circular leads with holes in the center of them for the snaps to connect through. First, the

male ends of the snap buttons are sanded down to roughly 2 mm using an S4S 4" Belt Sander (Kalamazoo Industries).

For the Al heating element, a wire is taped to each lead before the heating element is transferred from thermal release tape to 3M Tegaderm^{TM}. The Al circular leads are smaller than the Au circular leads because they only need to have enough surface area for the wire to be taped to. A hole is cut through the Tegaderm in the center of the leads using an X-Acto knife. The sanded male ends of the snap buttons are placed through the holes of each lead from the adhesive side of the Tegaderm. The female ends of the snap buttons are placed on top of the male ends and pressed into them using an arbor press (Drake 1.5 Ton Arbor Press), thus clamping the wires and the Al leads together securely between the ends of the snaps.

For the Au RTD, a wire is soldered to the top of the female end of the snap button for each lead. The sanded male ends of the snap buttons are placed through the holes of each lead from the adhesive side of the Tegaderm. The soldered female ends of the snap buttons are placed on top of the male ends and pressed into them using the arbor press, thus securing the bottom of the female snap button to the Au circular lead. The Au circular leads are bigger than the Al ones as to give the snap button more surface area to be in contact with the Au over.

With these wires securely connected to the heating element and RTD, the device can be connected to using standard alligator clips. A blown-up schematic of these connection set-ups can be seen in Figure 3A and B.

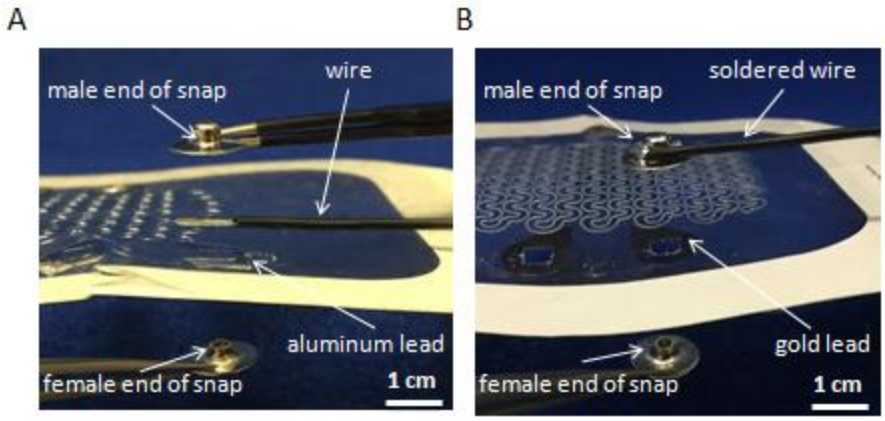

Figure 3: A) Connection components for the gold connections. Wire is soldered to the stud, eyelet is sanded down to 2 mm and put through the gold after gold has been transferred to the tegaderm, and then the stud is pressed onto the eyelet. B) Connection components for the aluminum connections. Wire is taped to the aluminum, and then aluminum is transferred to tegaderm. Eyelet is sanded down to 2.5 mm and put through the aluminum, and then the stud is pressed onto the eyelet.

Finally, a double-sided tattoo-adhesive is laid on top of the heating element and the RTD, providing a final layer of electrical insulation as well as increased adhesiveness to the patch.

HOT-PLATE CALIBRATION

A hotplate (Fisher Scientific Isotemp Digital HotPlate Stirrer 11-200-49SH) was covered with a graphite sheet to facilitate lateral heat distribution and 3M Micropore tape to provide electrical insulation. The RTD was placed on the hotplate along with two custom made type T thermocouples. The hotplate was then set to multiple settings. At each setting, the resistance of the RTD and the temperature of the hotplate were measured using an ohmmeter (Fluke 87) and the thermocouples, respectively (Figure 4A). The resulting calibration curve was linear with a fixed intercept slope of .002504 (Figure 4B).

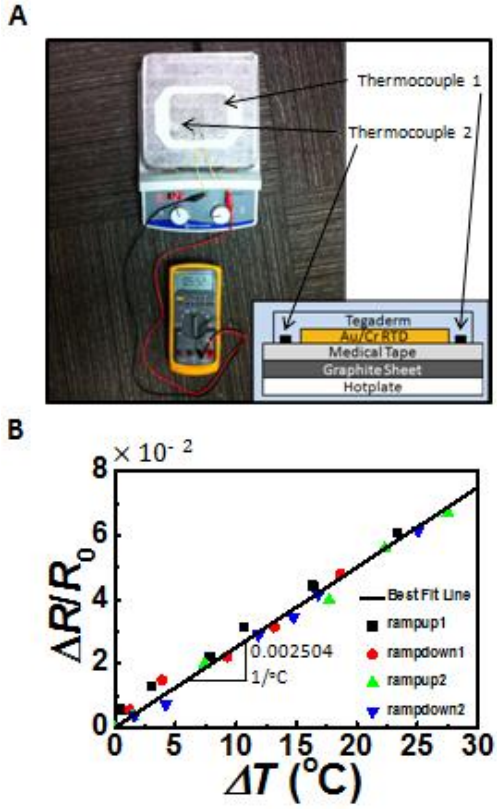

Figure 4: A) Set up for hotplate calibration of the RTD. Hotplate is lined with graphite to facilitate uniform lateral heat distribution and then medical tape for electrical insulation. Two thermocouples are placed on the hotplate, and a tegaderm patch with a gold RTD on it is put onto the hotplate. The resistance of the RTD is measured using a multimeter. The hotplate is set to various temperatures, and the resistance of the RTD and the temperatures of the thermocouples are recorded simultaneously. The inset shows a cross-sectional diagram of the set-up. B) The calibration curve for the RTD: $\Delta R/R_0$ of the RTD vs. ΔT of the average temperature of the two thermocouples measured twice while ramping the temperature up and twice while ramping the temperature down. There is no visible hysteresis. A calibration curve is plotted as a line of best fit through the points, and the calibration constant, β, is marked and is equal to .002504.

CALIBRATION ON GLASS

The RTD was then calibrated on an 18 in. x 18 in. x 0.3 in. slap of glass under the conditions that it would be subject to when used as part of the device. Glass was chosen

because it has thermal properties similar to that of skin[8]. Since the heat would be coming from the heating element and not a uniform hotplate, we hypothesized that the resistance of the RTD would change differently with the temperature of the heating device than it did with the temperature of the hotplate. The calibration set-up is shown in Figure 5.

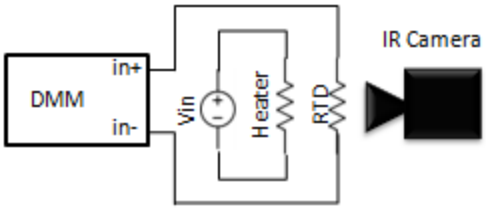

Figure 5: Circuit diagram of set-up for calibration of RTD in situ. Heater is brought to different temperatures by adjusting Vin. Resistance and temperature are measured simultaneously using DMM and IR camera, respectively.

The heating element was attached to a DC voltage supply (Mastech Linear Power Supply HY1803D), while the RTD was attached to a digital multimeter (DMM), specifically the NI Elvis II. Resistance readings were logged using LabVIEW 2014. The device was covered with a fine layer of Johnson's Baby Powder to increase its emissivity.[32] The DC voltage supply was set to 7.3V, and the temperature and resistance of the RTD were measured simultaneously using an IR camera (FLIR SC305) and the DMM, respectively. The IR camera was set to measure the maximum temperature that the heater reached. The heater reached the desired temperature of around 40^{o}C, and had a fairly even distribution (Figure 6A). The RTD was found to exhibit a linear relationship between its resistance and the maximum heater temperature (Figure 6B), but with a slightly lower thermal coefficient, as expected.

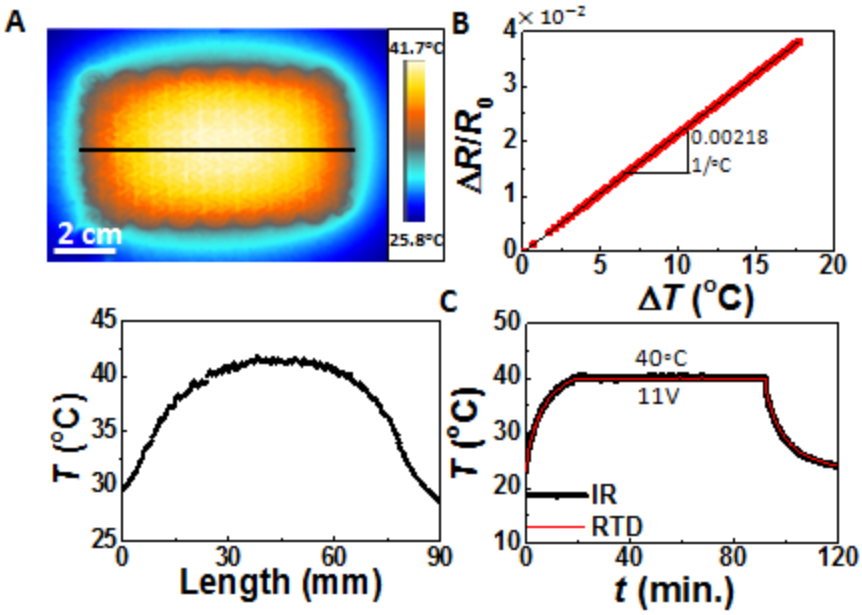

Figure 6: A) Top: IR image of the heater on a 0.3 in. thick slab of glass. Bottom: lateral heat distribution as measured across the black line indicated in the IR image. B) $\Delta R/R_0$ of the RTD vs. ΔT of maximum temperature of the heater. The calibration constant, β, is marked and is equal to .00218. C) Temperature of the heater on glass vs. time measured with both the RTD and the IR camera as the heater is turned on at a setpoint of 40°C and then turned off. Heater is able to maintain setpoint temperature for an extended period of time.

PID TEST ON GLASS

With the RTD calibrated, the heater was set up to work with PID control (Figure 7). The DC power to the heater was routed through an Omron DC-DC relay (G3CN) which was controlled by a computer using an output DAQ (NI USB-6009). The computer ran a LabVIEW program which controlled the heat of the heater using pulse width modulation (PWM). The RTD was connected to the DMM from before which fed its resistance to the LabVIEW program. The program converted the resistance readings into temperature using the thermal coefficient found in the calibration step. It then used that temperature feedback, along with a desired temperature set point, in a PID algorithm to

determine how to control the relay and thereby what power to supply to the heating device. This allowed the program to keep the heater at a desired temperature.

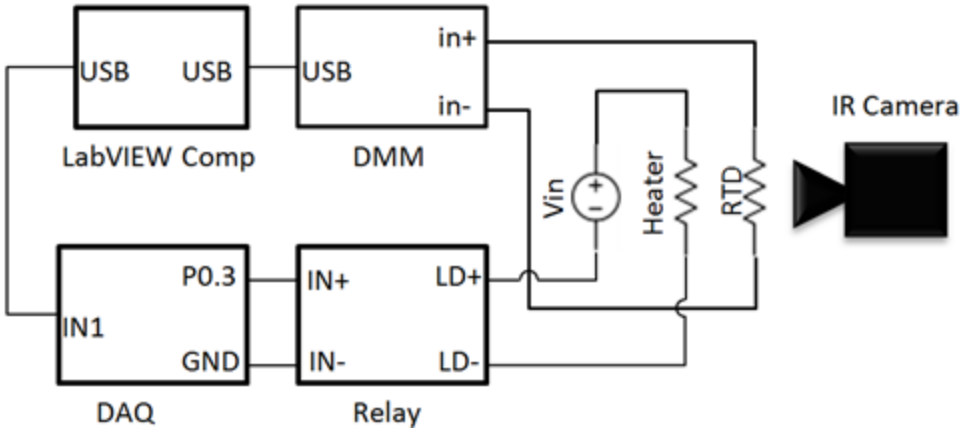

Figure 7: Circuit diagram of set up for operating heater with PID control. DMM measures resistance of RTD and feeds it into a computer with LabVIEW, The LabVIEW program calculates the temperature of the RTD using the RTD's starting temperature, starting resistance, and calibration constant. It then uses a PID algorithm to calculate the optimal duty cycle for PWM of the heater given the heater's current temperature and the setpoint temperature for the heater. The LabVIEW program then uses the DAQ to switch the relay on and off with the determined duty cycle, thus controlling how much total power is fed to the heater.

When run using PID feedback control with a setting of 40°C and a voltage supply of 11V, the heater was able to reach a temperature of 40°C and maintain the temperature consistently for over 40 minutes (Figure 6C).

MATERIALS AND METHODS CONCLUSION

The fabrication methods presented here resulted in a fully functioning heating device. This initial testing on glass showed promising results which were consistent enough to merit testing on humans without a significant safety risk. With the calibration method and PID circuit set-up designed and established, I was ready to find results from tests on humans with the heater.

Chapter 3: Results and Discussion

In this section I present the results from tests conducted with the heater. I will present the results of the conformability of the heater, the heat distribution on the skin, the thermal temperature coefficient of the RTD with regards to the average temperature of the heater, the ability of the heater to accurately measure temperature and maintain the device at a desired temperature, and the power density of the heater and how it compares to that of other heaters, and the stretchability of the heater.

CONFORMABILITY

When attached to the skin, this device conforms completely to the skin and bends with it (Figure 8A and B). When a DC voltage supply of 6V is attached across the aluminum heating element, the heater supplies an even amount of heat around the target temperature of 40^{o}C. The heater remains bendable during heating (Figure 8C and D).

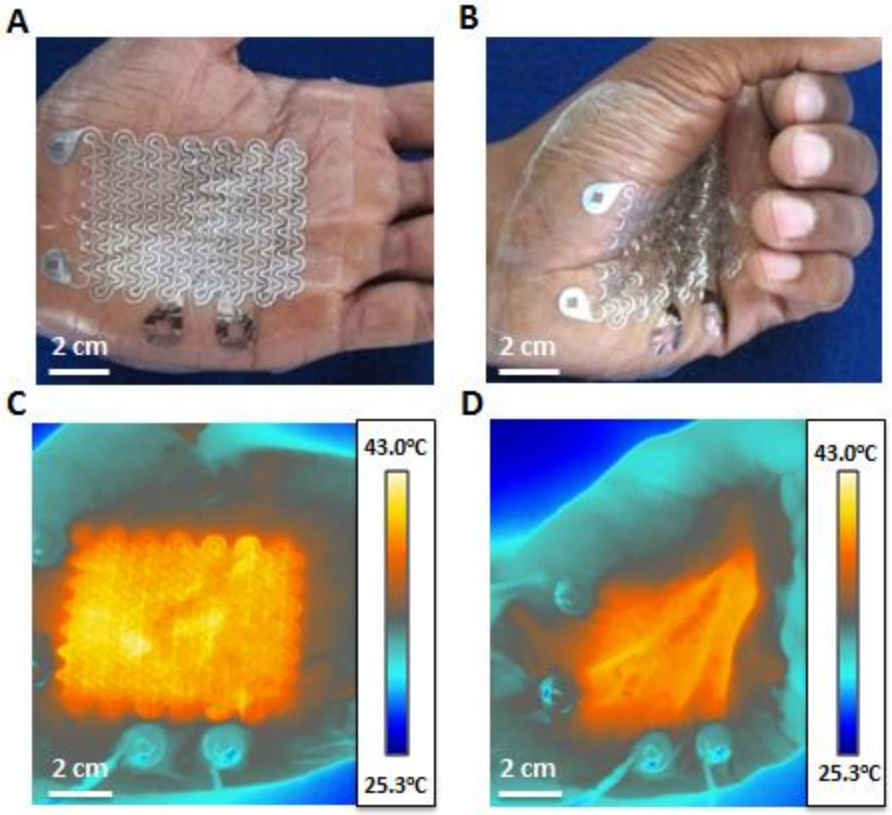

Figure 8: A and B) Device conforms to hand and maintains its conformability during opening and closing. C and D) IR images of the device powered with PID control as the hand is opened and closed. PID controller automatically adjusts power output so the hand does not overheat when it closes.

CALIBRATION ON SKIN

The RTD was then calibrated on skin under the conditions that it would be subject to when used as part of the device using the calibration set-up shown previously in Figure 5. The heating element was attached to a DC voltage supply, while the RTD was attached to a digital multimeter (DMM), specifically the NI Elvis II. Resistance readings were logged using LabVIEW 2014. The device was covered with a fine layer of Johnson's Baby Powder to increase its emissivity[32]. The DC voltage supply was set to different voltages, and the temperature and resistance of the RTD were measured simultaneously

using an IR camera (FLIR T620) and the DMM, respectively. Temperature readings from the IR camera were logged using FLIR Tools +.

The heater was found to be able to reach high temperatures and have a fairly uniform heat distribution. Figure 9A shows the IR image of the heater. The dotted square indicates the position of the RTD and the area whose average temperature was logged by the IR camera to get the IR temperature. The three horizontal lines across the heater mark the locations where the temperature was recorded and plotted as a function of distance across the line. As can be seen from the figure, the temperature of most of the heater stays consistently between 38^{o}C and 40^{o}C. The DC voltage was set to 3 different settings for this calibration: 3.8V, 4.5V, and 5.1V. The resulting temperature and resistance vs. time can be seen in Figure 9B. The temperature and resistance line up very well. Plotting resistance vs. temperature, we get a linear fit with a thermal coefficient of 0.00203 (Figure 9C). As expected, this is lower than the thermal coefficient found with the hotplate calibration (.0025) due to the fact that the heat from the heater is not as uniform as the hotplate, with a higher heat concentration towards the center.

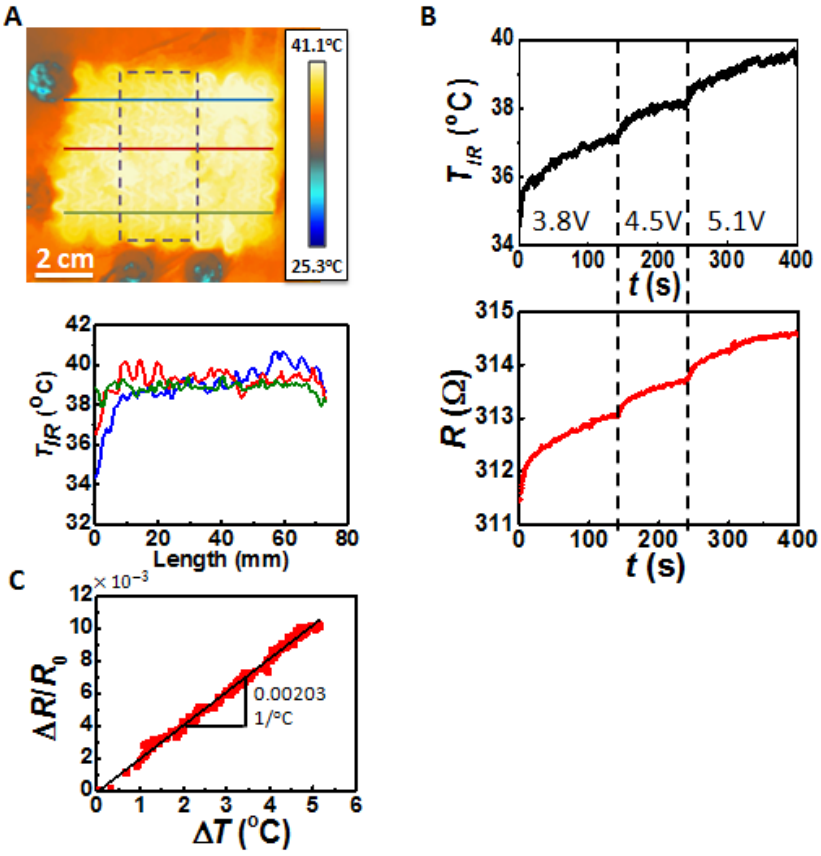

Figure 9: A) Lateral heat distribution of heater. Blue, red, and green lines on IR image mark the horizontal line across which temperature was measured for their respective red, blue and green plots. Temperature distribution is fairly uniform. Dotted purple line on IR image shows area that the IR camera calculated the average temperature for. B) Average temperature of area marked by the dotted purple line in Fig. 3B (top) and resistance of Au/Cr RTD as measured by DMM (bottom) each plotted across time as Vin was changed to 3.8V, 4.5V, and finally 5.1V. C) The calibration curve for the RTD: $\Delta R/R_0$ of the RTD vs. ΔT of the average temperature of the area around the RTD as marked by the dotted purple line in Fig. 3B. The calibration constant, β, is marked and is equal to 0.000203.

PID CONTROL ON SKIN

With the RTD calibrated, the heater was set up to work with the same PID control set-up as before (Figure 7). The computer ran a LabVIEW program which controlled the heat of the heater using pulse width modulation (PWM). The RTD was connected to the DMM from before which fed its resistance to the LabVIEW program. The program converted the resistance readings into temperature using the thermal coefficient found in the calibration step. It then used that temperature feedback, along with a desired temperature set point, in a PID algorithm to determine how to control the relay and thereby what power to supply to the heating device. This allowed the program to keep the heater at a desired temperature. The DC voltage supply was then set to 6.2V, and the temperature set point was set to 38.5^{o}C. The device was able to maintain a constant temperature of 38.5^{o}C for over 30 minutes, and the temperature readings of the RTD remained accurate as verified by IR camera measurements (Figure 10A).

A similar test was conducted next, but the temperature set-point was set to multiple different settings (37 ^{o}C, 38.5 ^{o}C, 40 ^{o}C) while the voltage supply was kept the same at 6.2V (Figure 10B). The voltage had to be increased for the final setting, as 6.2V was not enough voltage to power the heater up to 40 ^{o}C, even when the duty cycle of the PWM was at a constant of 100%. After the voltage was increased, the heater was able to maintain the desired set point temperature. For the first two temperatures, the device was able to reach the set temperatures and maintain them at a steady state. In switching between these temperatures, no changes were made except the LabVIEW program's set point. This result shows that our device, when given a large enough base voltage supply, can reach, maintain, and change between desired temperatures without any manual

adjustment of the voltage or any knowledge of the relationship between voltage supplied to the heater and temperature reached by the substrate for a given heater and substrate.

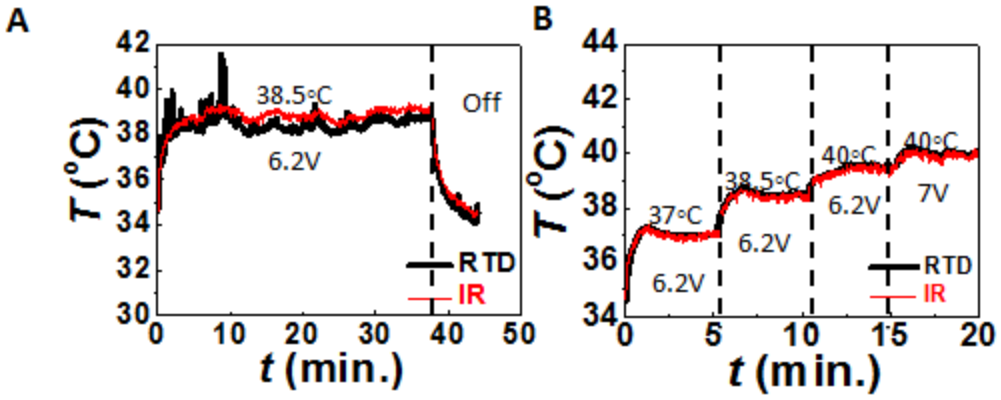

Figure 10: A) Temperature of the heater vs. time measured with both the RTD and the IR camera as the heater is turned on at a setpoint of 38.5°C and then turned off. Heater is able to maintain setpoint temperature for an extended period of time. B) Temperature of the heater vs. time measured with both the RTD and the IR camera as the setpoint of the heater is changed while the voltage remains constant. At 40°C, 6.2V is not sufficient for the heater to reach the setpoint, so the voltage is increased to 7V, at which point the heater is able to reach and maintain a temperature of 40°C.

POWER DENSITY CALCULATIONS

To analyze the power consumption of the heater, the device was set up with PID control at multiple different temperature settings. At each setting, the steady state duty cycle was recorded. This was used to calculate the power consumption of the heater using the following equation:

$$P = \frac{D}{100\%} * \frac{V^2}{R} \quad (2)$$

Where D is the duty cycle of the device, V is the voltage used to power the device, and R is the resistance of the Al heating element. After the power was calculated for each temperature, the power density for each temperature was calculated using the equation:

$$\text{Power Density} = P/A \tag{3}$$

Where A is the area of the heater. Linear least squares regression was then applied to the power densities with respect to their temperatures to estimate the mW/(cm^2•°C) of the heater (Figure 11A). The estimated value for this parameter was 0.846 mW/(cm^2•°C).

It is inaccurate to assume that all the power input into the heater is also input into the body, as much of the heater's heat is lost to the environment. In order to get a better approximation of how much power the heater was able to put into the body at each temperature, the entire experiment was repeated but with a 3cm thick layer of foam held lightly against the device by hand (Figure 11B). Under these conditions, the power input into the body was calculated as 0.784 mW/(cm^2•°C).

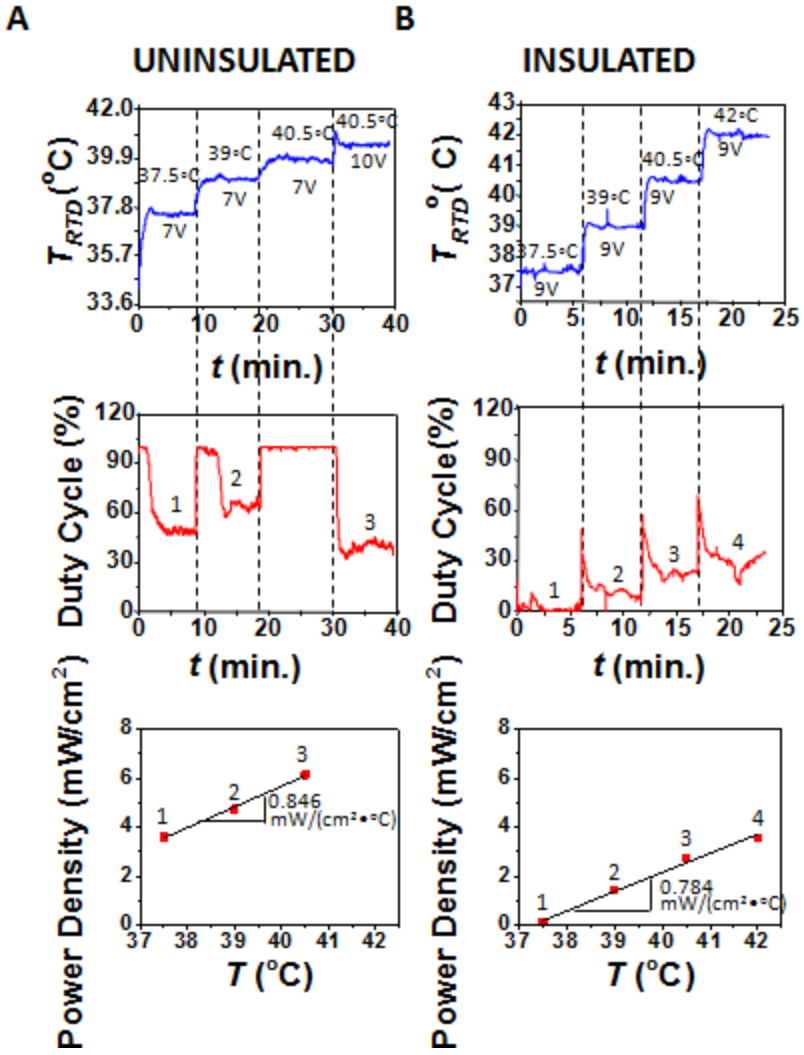

Figure 11: A) Plot of heater temperature vs. time as the setpoints and voltages are changed, followed by a plot of the corresponding duty cycle vs. time. The average of the steady state duty cycles marked 1, 2, and 3 were used to calculate the power densities plotted below marked 1, 2, and 3, respectively, at different temperatures. B) The same plots as figure A except the heater is insulated with a piece of foam.

Using Equations (2) and (3), power consumption values were calculated for other stretchable heaters. These results, along with other information about the heaters and what substrates they were on for which these values were reported, are included in Table

1. In cases where power to heater was direct and not pulse width modulated, the value of D was set to 100%. We see that the power consumption of our device is comparable to that of other stretchable heaters.

Ref	T sensor on site	Feedback Control	Target T (°C)	Material	Substrate	V (V)	R (Ω)	Area (cm^2)	P (W)	Power Density (mW/cm^2)	($mW/(cm^2 \cdot °C)$)
Our device	Yes	Yes	43	Al	Skin	10	17.2	38.7	2.38	61.44	0.85
[4]	No	No	43	LE Ag NW/SBS (18/32)	Skin	3.7	18.3	91	0.74	8.18	0.82
[28]	No	No	39	Ag/PDMS NW 132 mg m^{-2}	Air	4	50	38.5	0.32	8.31	0.64
[28]	No	No	56	Ag/PDMS NW 396 mg m^{-2}	Air	5	15	38.5	1.67	43.29	1.02
[33]	Yes	No	37	Cr/Au 7/70nm	PDMS	4.4	550	9	0.04	3.91	0.78
[14]	Yes	Yes	42	Cr/Au 10/190nm	1mm thick glass slide	12	95.9	0.18	1.50	8342.02	490.00
[29]	Yes	No	ΔT = 6	Au	Skin			0.64	0.01	20.31	3.39

Table 1: Power consumptions of different heaters from literature.

STRETCHABILITY

An RTD was fabricated on Tegaderm and placed into a customized tensile tester. The resistance of the RTD was measured using a digital multimeter (Rigol DM3068) as the RTD was stretched to a strain of 70% (Figure 12a) and relaxed back to a strain of 0% three times. The results are plotted in Figure 12b. As can be seen, the normalized change in resistance of the RTD increases consistently with an increase in strain and decreases

consistently with a decrease in strain. Since the LabVIEW program measuring and controlling the heating device interprets an increase in resistance as an increase in temperature according to the thermal coefficient found during the calibration step, we hypothesized that bending the hand would cause the program to overestimate the temperature of the device due to the increase in strain of the RTD.

To examine the overall impact of this phenomenon on the behavior of the device during use, a full device was fabricated and placed on a male human subject's hand. The device was set up according to the schematic in Figure 5: the heater was powered with a constant voltage of 3.8V directly without any feedback control, the RTD was connected to a digital multimeter (NI Elvis II), and the device was recorded with an IR camera (FLIR T620). The subject closed his hand as much as he could without blocking the line of sight of the IR camera and opened it again while the temperature of the hand was recorded with the RTD and the IR camera simultaneously. The resulting measurements can be seen in Figure 12B. Originally, when the hand is open, the RTD reads the correct temperature and matches the temperature readings of the IR camera. Once the hand closes, the temperature of the hand increases, likely due to the wires of the heater being brought closer together. However, the RTD reads a much higher temperature increase than is accurate, as we hypothesized. Once the hand opens up again, the temperature of the hand returns to its original temperature. The RTD reading becomes much more accurate, but it still overestimates the temperature slightly. This indicates that there is some permanent resistance increase in the RTD from closing the hand that is not undone when the hand opens again.

The device was then set up according to Figure 7 and set-up to work with PID control at a setting of 40°C and a voltage supply of 10V. The hand was closed and opened twice in a fashion similar to that of the previous experiment. The temperature reading results can be seen in Figure 12C. When the hand closes, the RTD overestimates the temperature of the device, and the controller responds by decreasing the temperature of the heater. When the hand opens again, the RTD reads the correct temperature, and the controller increases power to the heater to bring its temperature back up to 40°C. Again, there is some lasting inaccuracy after the hand opens again, indicating that closing the hand causes some permanent resistance increase in the RTD.

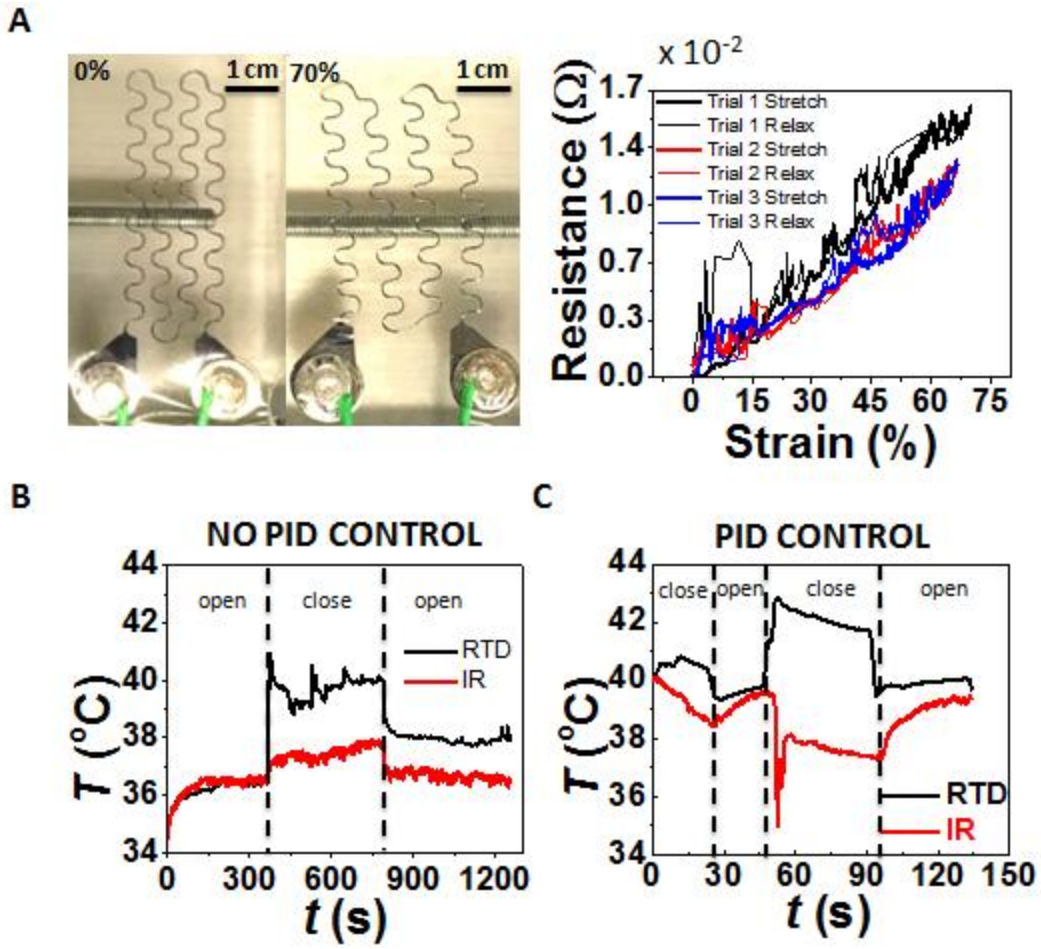

Figure 12: A) Strain test for RTD. RTD on tegaderm is placed into stretching device and the resistance of the RTD is measured with a DMM as the RTD is stretched. The resistance vs. strain is plotted. This shows that the resistance increases with strain. B) Temperature of the heater powered with a constant voltage and no PID control as the hand opens and closes measured using the IR device and the RTD and plotted vs. time. When the hand closes, the RTD measures a false increase in temperature due to the strain induced on the RTD. C) Temperature of the heater powered with PID control as the hand opens and closes measured using the IR device and the RTD. When the hand closes, the controller cools down the heater to counteract the perceived increase in temperature. When the hand opens again, the RTD and the IR measurements agree again, and the controller heats up the heater to counteract the cooling that occurred when the hand was closed.

RESULTS CONCLUSION

The fact that the heater is able to consistently able to maintain a given temperature without any knowledge of the relationship between the voltage applied to the heater and the temperature the heater will reach on whatever surface it is on means that it can be applied to any part of the body on any human and should be able to function normally. This is something that cannot be said for other stretchable heaters. In fact, this device should be able to function well on surfaces that are not human skin, providing that the temperature distribution is similar enough that the RTD will exhibit the same relationship between temperature of the heater and resistance of the RTD. The heater can reach very high temperatures without forming hot-spots and meets criteria to be used in applications listed previously such as thermal joint therapy, perioperative warming, and drug release control.

The stretchability results of the heater indicate that in order for it to work properly, the surface it is on will have to not bend too much. However, the fact that the RTD overestimates temperature and does not underestimate it means that the device will error on the side of providing too little power instead of too much, which means the device does not pose a safety threat of overheating the skin due to flawed temperature readings.

The power consumption of the heater is very reasonable. It is worth noting that the voltage needed to power the heater to specific temperatures is significantly higher when the voltage supply is routed through the DC-DC relay, suggesting that a significant amount of power is lost to the relay. The power consumption of the device could be even lower if a relay with less power consumption was used. Also, the test with the heater run under insulation is one that has not been run before with other stretchable heaters, in large part because the test is not possible without an on-site temperature sensor. Thus this test

provides novel insight to the power absorbed into the skin from a stretchable heating device.

Chapter 4: Conclusion

Heaters which can be applied to human skin are important for a variety of applications, including perioperative warming, drug acceleration, and thermal joint therapy. Existing heaters either cannot safely reach high enough temperatures or, in the case of forced air warming, are very bulky and obstructive and do not work as efficiently as would be ideal. Many flexible heating devices have been developed which could serve as a useful alternative to these heaters. These flexible heaters can conform and adhere to the skin completely, allowing for the heat to reach high temperatures without danger of hotspots forming and causing burns. These heaters, however, are expensive or tedious to make. Moreover, none of them utilize a temperature feedback control system, and must therefore rely on a known voltage to temperature relationship in order to power the heater to the desired temperature. This relationship may vary due to biological conditions.

The smart epidermal heater presented in this thesis integrates both stretchable heater and RTD on the same patch. It is low-cost and simple to produce, and it uses PID temperature feedback control to maintain a desired temperature. The heating element is able to reach high temperatures with a relatively even distribution. The RTD successfully monitors the real time, true temperature of the epidermis, as verified through IR measurements. The device has low power consumption compared with other state-of—the-art flexible heaters. The device is able to maintain set temperatures for extended

periods of time, and can automatically adjust to a different temperature if the temperature setting is changed.

This heater solves many problems of present heaters and can be useful for the listed applications. Its simple circuit and program can easily be downscaled to a battery powered PCB and microcontroller, giving it potential for point-of-care applications. The cut-and-paste manufacturing process is robust enough that the heater and RTD can be made in different shapes and sizes or out of different materials and incorporated with different stretchable substrates. I have demonstrated how to effectively synergize a stretchable RTD and stretchable heater in a way that generalizes beyond my device specifically, as the methods are not specific to the shape and size of the device. In fact, the fabrication methods listed can be used to stack other epidermal electronic devices on top of each other besides a heater and an RTD. Some examples of other devices that could be overlayed in this fashion include hydration sensors, EEG sensors, ECG sensors, and EMG sensors, all of which have been created using the cut-and-paste method before by Yang et. al. I have also quantified the effects of insulating a skin-laminated epidermal heater from the ambient environment. We hope that these innovations and findings spur increased growth in stretchable devices and specifically epidermal heaters for medical applications.

There is a significant amount of future work that could be done in this area, and specifically with this device. The device presented in this paper only uses one RTD, but it would be very possible to use multiple RTDs and thus get a better and more full characterization of the temperature field of the epidermis. This would allow the heater to respond to specific scenarios such as the occurrence of local hot spots.

Improving the cable connections and prestretching the RTD before calibration could reduce the inaccuracy that the RTD develops after mechanical deformation. Stiff polymers can be used to encapsulate the miniaturized RTD into a stiff island such that its temperature readings will not increase with strain[29]. If a method of doing this can be found that is compatible with the cut-and-paste method, it would greatly increase the deformation immunity of the device.

Test methods from a paper by Choi et. al.[4] could be replicated to determine how well the device will work for thermal joint therapy. To confirm the effectiveness of the heater for perioperative warming, the heater can be placed on the hand of someone who is vasodilated. The power input into the body under these conditions can be monitored, and it can be confirmed that the device is able to maintain the set temperature. As an initial the test, the device can be places on a tube with water circulating through it, which would model the blood carrying away the heat input from the heater.

To experiment with drug release from the heater, methods from Son et. al.[14] or Bagherifard et. al.[34] can be adopted to fabricate medical patches which release drugs when heated. However, the heater may need an extra layer of waterproof protection in order to stay adhered during the release of drugs if they are watery.

This cut-and-paste heater with an on-site RTD could open up new possibilities in heater design for medical applications, and I hope that we will see continued growth in the field of stretchable electronic heaters.

References

1. Brosseau, L. *et al.* in *Cochrane Database of Systematic Reviews* (John Wiley & Sons, Ltd, 2003).
2. Roos, E. M. Joint injury causes knee osteoarthritis in young adults. *Curr. Opin. Rheumatol.* **17,** 195–200 (2005).
3. Lehmann, J. *Therapeutic heat and cold*. (Williams & Wilkins, 1990).
4. Choi, S. *et al.* Stretchable Heater Using Ligand-Exchanged Silver Nanowire Nanocomposite for Wearable Articular Thermotherapy. *Acs Nano* **9,** 6626–6633 (2015).
5. Petrofsky, J. S., Laymon, M. & Lee, H. Effect of heat and cold on tendon flexibility and force to flex the human knee. *Med. Sci. Monit. Int. Med. J. Exp. Clin. Res.* **19,** 661–667 (2013).
6. Sessler, D. I., Rubinstein, E. H. & Moayeri, A. Physiologic responses to mild perianesthetic hypothermia in humans. *Anesthesiology* **75,** 594–610 (1991).
7. Grahn, D., Brock-Utne, J. G., Watenpaugh, D. E. & Heller, H. C. Recovery from mild hypothermia can be accelerated by mechanically distending blood vessels in the hand. *J. Appl. Physiol. Bethesda Md 1985* **85,** 1643–1648 (1998).
8. Roselli, R. J. & Diller, K. R. *Biotransport: Principles and Applications*. (Springer, 2011).
9. Diller, K. R. Heat Transfer in Health and Healing1. *J. Heat Transf.* **137,** 103001–103001 (2015).

10. Cartmell, J. V. & DeRosa, J. F. Capacitively coupled indifferent electrode. (1987).
11. Shi, H.-X. *et al.* The Anti-Scar Effects of Basic Fibroblast Growth Factor on the Wound Repair In Vitro and In Vivo. *Plos One* **8,** e59966 (2013).
12. Galiano, R. D. *et al.* Topical vascular endothelial growth factor accelerates diabetic wound healing through increased angiogenesis and by mobilizing and recruiting bone marrow-derived cells. *Am. J. Pathol.* **164,** 1935–1947 (2004).
13. Bagherifard, S. *et al.* Hydrogel based dermal patch with integrated flexible electronics for on demand drug delivery. in *ResearchGate* (2014).
14. Son, D. *et al.* Multifunctional wearable devices for diagnosis and therapy of movement disorders. *Nat. Nanotechnol.* **9,** 397–404 (2014).
15. Michlovitz, S., Hun, L., Erasala, G. N., Hengehold, D. A. & Weingand, K. W. Continuous low-level heat wrap therapy is effective for treating wrist pain. *Arch. Phys. Med. Rehabil.* **85,** 1409–1416 (2004).
16. Tuckey, J. Forced-air warming blanket and surgical access. *Anaesthesia* **54,** 97–98 (1999).
17. Kimberger, O. *et al.* Resistive Polymer Versus Forced-Air Warming: Comparable Heat Transfer and Core Rewarming Rates in Volunteers: *Anesth. Analg.* **107,** 1621–1626 (2008).
18. Sekitani, T. *et al.* A Rubberlike Stretchable Active Matrix Using Elastic Conductors. *Science* **321,** 1468–1472 (2008).
19. Jung, S. *et al.* Reverse-Micelle-Induced Porous Pressure-Sensitive Rubber for Wearable Human–Machine Interfaces. *Adv. Mater.* **26,** 4825–4830 (2014).

20. Chun, K.-Y. *et al.* Highly conductive, printable and stretchable composite films of carbon nanotubes and silver. *Nat. Nanotechnol.* **5,** 853–857 (2010).
21. Ma, R., Lee, J., Choi, D., Moon, H. & Baik, S. Knitted Fabrics Made from Highly Conductive Stretchable Fibers. *Nano Lett.* **14,** 1944–1951 (2014).
22. Park, M. *et al.* Highly stretchable electric circuits from a composite material of silver nanoparticles and elastomeric fibres. *Nat. Nanotechnol.* **7,** 803–809 (2012).
23. Moon, G. D. *et al.* Highly Stretchable Patterned Gold Electrodes Made of Au Nanosheets. *Adv. Mater.* **25,** 2707–2712 (2013).
24. Kim, Y. *et al.* Stretchable nanoparticle conductors with self-organized conductive pathways. *Nature* **500,** 59–63 (2013).
25. Yang, S., Ng, E. & Lu, N. Indium Tin Oxide (ITO) serpentine ribbons on soft substrates stretched beyond 100%. *Extreme Mech. Lett.* **2,** 37–45 (2015).
26. Kim, D.-H. *et al.* Epidermal Electronics. *Science* **333,** 838–843 (2011).
27. Fan, J. A. *et al.* Fractal design concepts for stretchable electronics. *Nat. Commun.* **5,** 3266 (2014).
28. Hong, S. *et al.* Highly Stretchable and Transparent Metal Nanowire Heater for Wearable Electronics Applications. *Adv. Mater.* **27,** 4744–4751 (2015).
29. Webb, R. C. *et al.* Ultrathin conformal devices for precise and continuous thermal characterization of human skin. *Nat. Mater.* **12,** 938–944 (2013).
30. Aström, K. J. & Murray, R. M. *Feedback Systems: An Introduction for Scientists and Engineers*. (Princeton University Press, 2010).

31. Yang, S. *et al.* 'Cut-and-Paste' Manufacture of Multiparametric Epidermal Sensor Systems. *Adv. Mater.* **27,** 6423–6430 (2015).
32. Methods of Increasing Emissivity in the Infrared Spectrum. Available at: http://www.optotherm.com/emiss-increasing.htm. (Accessed: 2nd May 2016)
33. Kim, J. *et al.* Stretchable silicon nanoribbon electronics for skin prosthesis. *Nat. Commun.* **5,** 5747 (2014).
34. Bagherifard, S. *et al.* Dermal Patch with Integrated Flexible Heater for on Demand Drug Delivery. *Adv. Healthc. Mater.* **5,** 175–184 (2016).